LAND COVER IMAGE ENDMEMBERS IN AVIRIS IMAGERY IN THE NEUSE RIVER BASIN, NORTH CAROLINA[1]

Andrew Pilant,[2] Ross Lunetta,[2] Terrence Slonecker,[3] John Streicher,[4] and John Iiames[2]

1. INTRODUCTION

The U.S. Environmental Protection Agency (EPA) National Exposure Research Laboratory (NERL) is conducting hyperspectral remote sensing (imaging spectroscopy) methods development research in the Neuse River Basin, North Carolina. Science objectives have focused on the potential applications of hyperspectral imagery for vegetation discrimination in biologically diverse ecosystems. Imagery was collected by NASA's Airborne Visible/Infrared Imaging Spectrometer (AVIRIS) on July 20, 1999 along a single northwest-southeast oriented flight line in the Atlantic Coastal Plain between New Bern and Kinston, North Carolina. Overall research goals include the evaluation of well-characterized and high signal-to-noise AVIRIS data for vegetative community discrimination and to evaluate (simulation) the potential application of MODIS-based spectral unmixing for vegetation discrimination in the broader Albemarle-Pamlico Basin (APB).

The analysis presented here was directed at extracting a suite of AVIRIS-derived spectral image endmembers from a full scene and determining the land cover class of pixels belonging to each endmember. Image endmembers are the purest pixels in a scene, and can be used as reference spectra in spectral unmixing and land cover mapping. The sections that follow detail the reflectance calibration, the data reduction process, the interactive selection of endmembers, and the land cover class labeling of endmember pixels by comparison with a coregistered land cover / land use (LCLU) map. We close with a discussion of the resultant AVIRIS image endmembers and factors that contributed to endmember emergence from the background data.

2. DATA COLLECTION

The AVIRIS data system is described by Green, et al. (1998). One AVIRIS flight line was collected on July 20, 1999 (14:00 GMT) in the New Bern-Kinston stretch of the Neuse River, immediately upstream of the Neuse Estuary (Fig. 1). Aircraft motion geometric distortions are minimal. Minor haze and clouds (highlighted in images at 1882 nm) are considered negligible for this analysis. The single scene analyzed here (f990720t01p02_r02_sc06.v1.img) is dominated by agriculture and wetland forest flood plain, and is almost entirely vegetated, except for fallow agricultural fields, rivers, ponds, pavement and buildings.

---

[1] **Notice:** This paper has been reviewed in accordance with the U.S. Environmental Protection Agency's peer and administrative review policies and approved for presentation and publication. Mention of any trade names or commercial products does not constitute endorsement or recommendation for use.

[2] U.S. EPA National Exposure Research Laboratory, Landscape Characterization Branch, 79 T.W. Alexander Drive MD-56, Research Triangle Park, North Carolina 27711, pilant.drew@epa.gov

[3] U.S. EPA National Exposure Research Laboratory, Landscape Ecology Branch, Environmental Photographic Interpretation Center, 12201 Sunrise Valley Drive, 555 National Center, Reston, Virginia 20192

[4] National Oceanic and Atmospheric Administration, U.S. EPA National Exposure Research Laboratory, Landscape Characterization Branch, 79 T.W. Alexander Drive MD-56, Research Triangle Park, North Carolina 27711

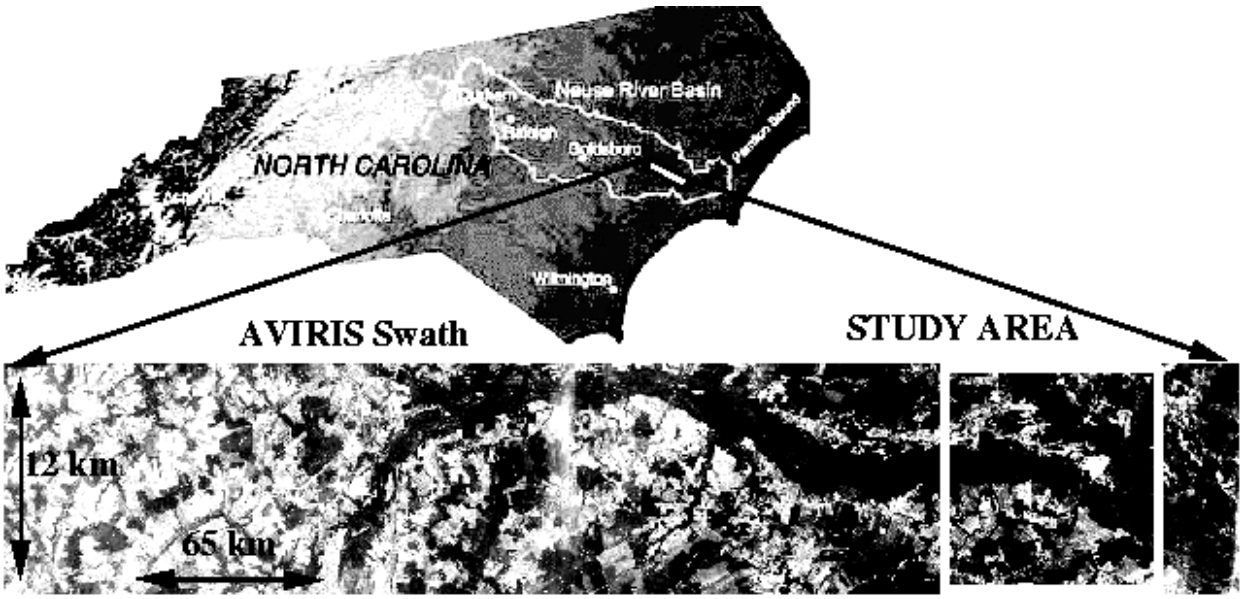

Figure 1. Location of AVIRIS swath and study area in the Neuse River Basin, North Carolina.

2.1 Field Spectroscopy

Fifteen close range field spectra were acquired on November 1-2, 2000 for calibrating the AVIRIS radiance data to apparent reflectance. Calibration targets were selected for optimal performance, i.e., homogenous materials, spectrally flat, time invariant, identifiable in the AVIRIS scene, and preferably spanning a range of low to high reflectance. Candidate pixels for light and dark calibration targets were first screened by examining images showing the darkest and brightest 20% of pixels at four wavelengths (459, 654, 1564, 2192 nm). Potential targets were identified in the northwest and southeast portions of the swath (those areas most anthropogenically developed): airport runway, factory rooftops, water treatment pond, soil baseball infield, and parking lots.

Field spectra were acquired using an Analytical Spectral Devices Full Range Field Spectrometer (Fig. 2) recording upwelling radiance from 350-2500 nm. The instrument was mounted on a tripod approximately 30 cm above the ground, sampling within a 2-4 m^2 region around a central point. Reference spectra of a calibrated Spectralon^{TM} tablet were collected before and after each 5 target spectra. The mean spectrum of five spectra for each target was used in the subsequent image calibration. Field site locations were measured with a Trimble TDC1 GPS in differential corrected mode, accurate to 1.0 m horizontal.

Figure 2. Field spectrometer, Spectralon tablet and GPS.

Atmospheric and solar conditions differed between the AVIRIS acquisition (July 20, 1999; 14:08 GMT) and field spectroscopy (November 1-2, 2000; 15:00-20:00 GMT). The July atmosphere was more humid than November, with visible haze and some cirrus clouds. The solar geometry was as follows: July (elevation: 48^o; azimuth 98^o); November (elevation: 36^o, azimuth: 155^o, 17:00 GMT).

2.2 Endmember LCLU Linkages

A recently compiled (U.S. EPA), remote-sensing based Neuse River Basin LCLU map was used to identify the land cover class of pixels identified as AVIRIS spectral image endmembers. The map was produced from 1998-99 SPOT 4 XS and Landsat 7 ETM$^+$ scenes, plus GIS input data (roads and wetlands). It has a pixel size of 15 m, with a 0.4 ha minimum mapping unit (MMU) (0.1 ha MMU in riparian zones). Overall Level I accuracy as verified

by a virtual field reference database[5] is 88% (n=1360 validation sites) with a Kappa statistic (KHAT) of 0.82 (n=1360).

3. AVIRIS DATA PROCESSING

The goal of the AVIRIS processing (Fig. 3) was to calibrate the raw AVIRIS radiance data to apparent surface reflectance, identify the most spectrally pure pixels, extract endmembers, and determine the class identity for each endmember based on the NRB LCLU map and visual interpretation of the AVIRIS imagery.

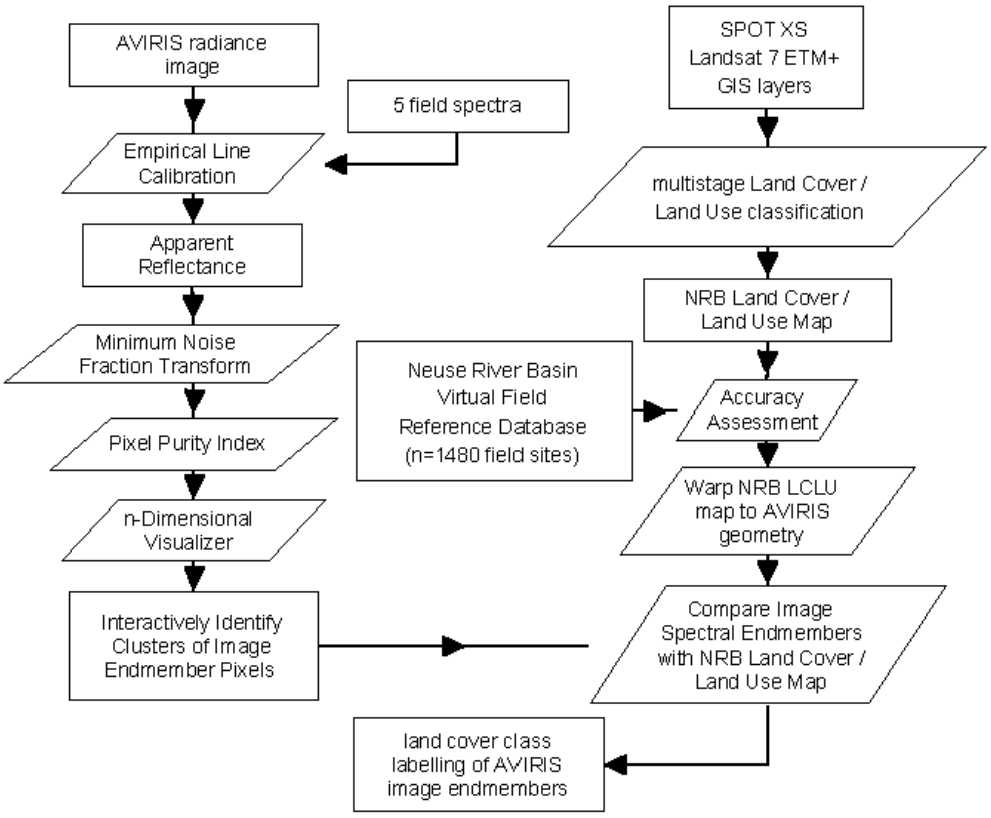

Figure 3. Flowchart of AVIRIS processing steps (left column).

3.1 Empirical Line Calibration

The technique used for calibrating radiance data to apparent reflectance was the Empirical Line Calibration method (Farrand, et al., 1994). A linear regression was performed to relate field spectra reflectance to AVIRIS radiance for corresponding pixels in the image. Generally, at least two field spectra are used: one bright and one dark target. Additional field spectra improve calibration quality.

Five field spectra were used in calibration of this scene: three factory roof targets, one gravel parking lot, and one pond. The gravel pixel and pond pixels were spectrally pure. However, it proved difficult to distinctly locate the roof targets in the image due to their limited areal extent and spectral similarity to surrounding pixels. It was necessary to use these roofs due to the absence of suitably large calibration targets in the scene. Fortunately, the surrounding roof and pavement pixels were spectrally similar, thus limiting the problem of mixed pixels. A scaling

[5] The Virtual Field Reference Database is available online at www.epa.gov/nerlesd1/lcb/nrb/VFRDB/

artifact was evident in the blue and green wavelengths, where reflectance dipped to negative 10%. This may have been due to a greater degree of Raleigh scattering under July sky conditions during the AVIRIS acquisition, relative to drier November sky conditions (less scattering) for the field spectra collection.

3.2 Minimum Noise Fraction Transform

The Minimum Noise Fraction (MNF) Transform is a sequence of two cascaded principal component transforms that results in a series of transformed bands ordered by decreasing signal to noise ratio (Green, et al., 1988; Boardman and Kruse, 1994). The analyst selects those bands with the highest signal-to-noise ratio (SNR) for further processing, and omits the remaining lower SNR bands. High SNR bands typically have eigenvalues > 1.0, and the images appear coherent, whereas the low SNR bands are dominated by noise (typically of a speckle nature). For this data set, the MNF image quality was significantly degraded for MNF bands 30 and greater (eigenvalues > 1.45)

3.3 Pixel Purity Index

MNF bands 1-30 were input to the Pixel Purity Index™ (PPI) algorithm (ENVI, 1999). The PPI algorithm finds the more spectrally pure pixels in scene by iteratively projecting the pixels onto a unit vector in n-dimensional space. Each time a pixel was found to be 'extreme', its count was increased by one. The output was an image with a PPI count assigned to each pixel. Then those pixels below some heuristically estimated threshold value were discarded to create a subset of the most spectrally pure pixels in the scene. This subset was then input to the n-Dimensional Visualizer™ algorithm (ENVI, 1999).

3.4 Interactive Selection of Image Endmembers

At this point in the processing flow the most spectrally pure pixels in the scene had been identified. Next, those pixels were interactively grouped to define image endmembers using an animated n-dimensional scatter plot (n-Dimensional Visualizer™ (*ibid*.)). Numerous bands were selected for input to the n-Dimensional Visualizer™ (three to six at a time generally worked well), then interactively grouped into clusters of pixels in a 3-D display using the mouse as the n-dimensional data cloud rotates on the computer screen. Through this process, 28 endmembers were extracted, with n=1 to 518 pixels (spectra) per endmember. Figure 4 graphs the mean spectrum of each endmember. Three endmembers were artifacts and were omitted from the discussion below. Figure 5 is a true color image of the AVIRIS scene showing color-coded locations of endmember pixels.

3.5 Determining LCLU Class of Image Endmembers

The land cover class of each endmember was determined by comparison with the coregistered cover type map. The NRB LCLU map was warped using ground control points to coregister with the unrectified AVIRIS scene (RMSE < 0.5 pixel). This preserved spectral fidelity by avoiding resampling reflectance values in a geometric warp. The analyst examined each pixel in each endmember, and noted the land cover class of the pixel as indicated by a) the NRB LCLU map and b) a true color composite of AVIRIS bands.

In many cases, multiple cover classes were captured by a single endmember; the dominant class(es) type determined the label. For example, endmember #3 contained 18 pixels distributed as follows: soy (11), cotton (2), pasture/hay (4), woody-mixed (1), and was labeled Agriculture- soy/pasture. In a similar manner, a label was applied to each endmember according to the dominant land class types indicated by the NRB LCLU map.

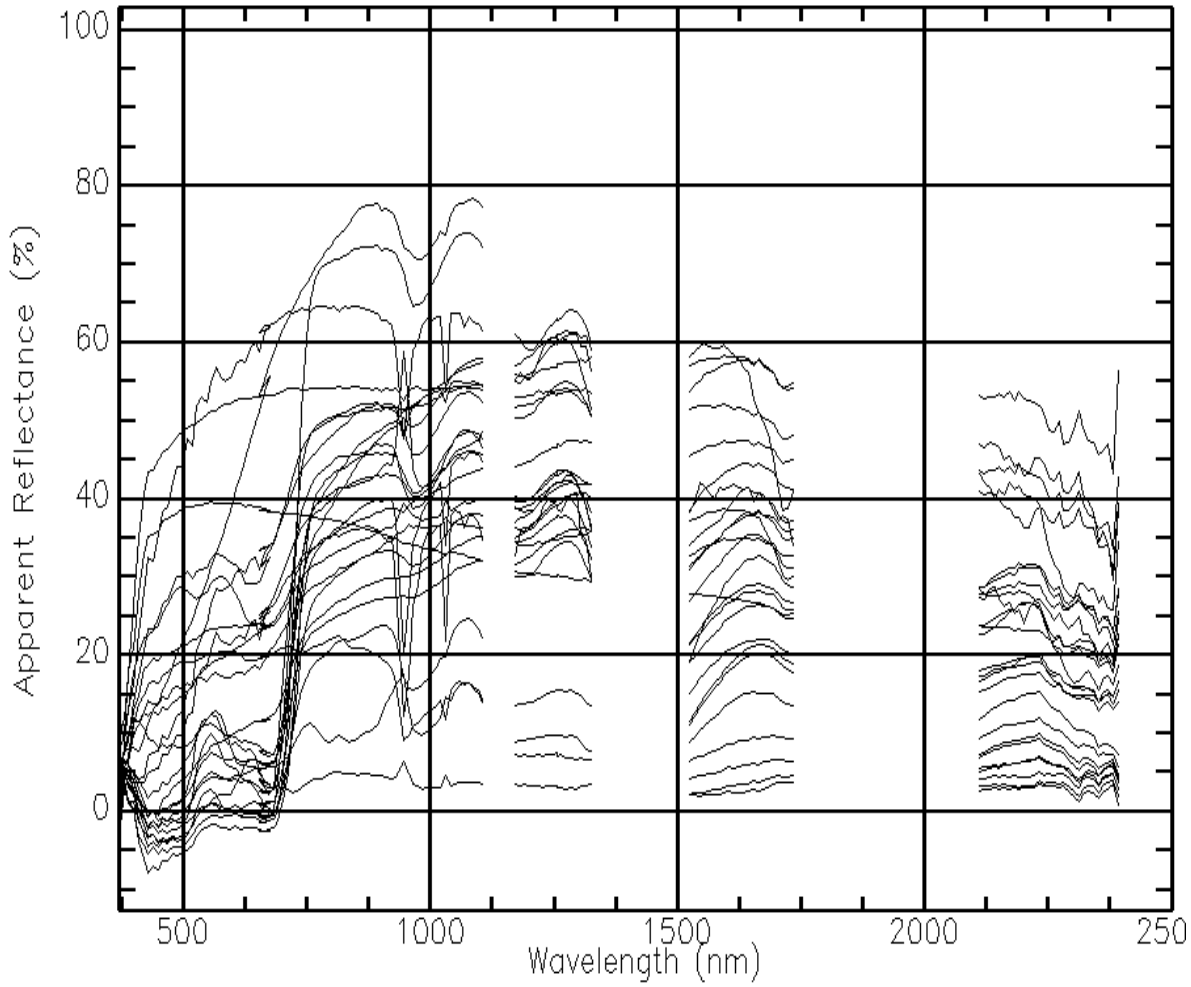

Figure 4. AVIRIS image endmember spectra. Each spectrum is the mean of all spectra for each endmember. The three Edge Artifact spectra are omitted.

4. RESULTS

The processing steps outlined in Figure 3 (left column) yielded 28 endmembers. They were distributed among the LCLU classes as follows:

- Urban (11 endmembers)
- Agriculture (9)
- Edge Artifacts (3)
- Mixed (2)
- Woody Vegetation (1)
- Water (1)
- water treatment pond Aerator Foam (1).

Figures 6-8 show example spectra for selected endmembers. Eleven endmembers were labeled urban. This class is defined as impervious surfaces plus unpaved roads (e.g., roofs (Fig. 6A), pavement, roads). Nine were labeled agriculture, and were further identified as cotton, corn, tobacco, soy or pasture. Most vegetation endmember spectra exhibited a green peak, red edge and near infrared plateau. Some appeared to be mixed with urban spectra

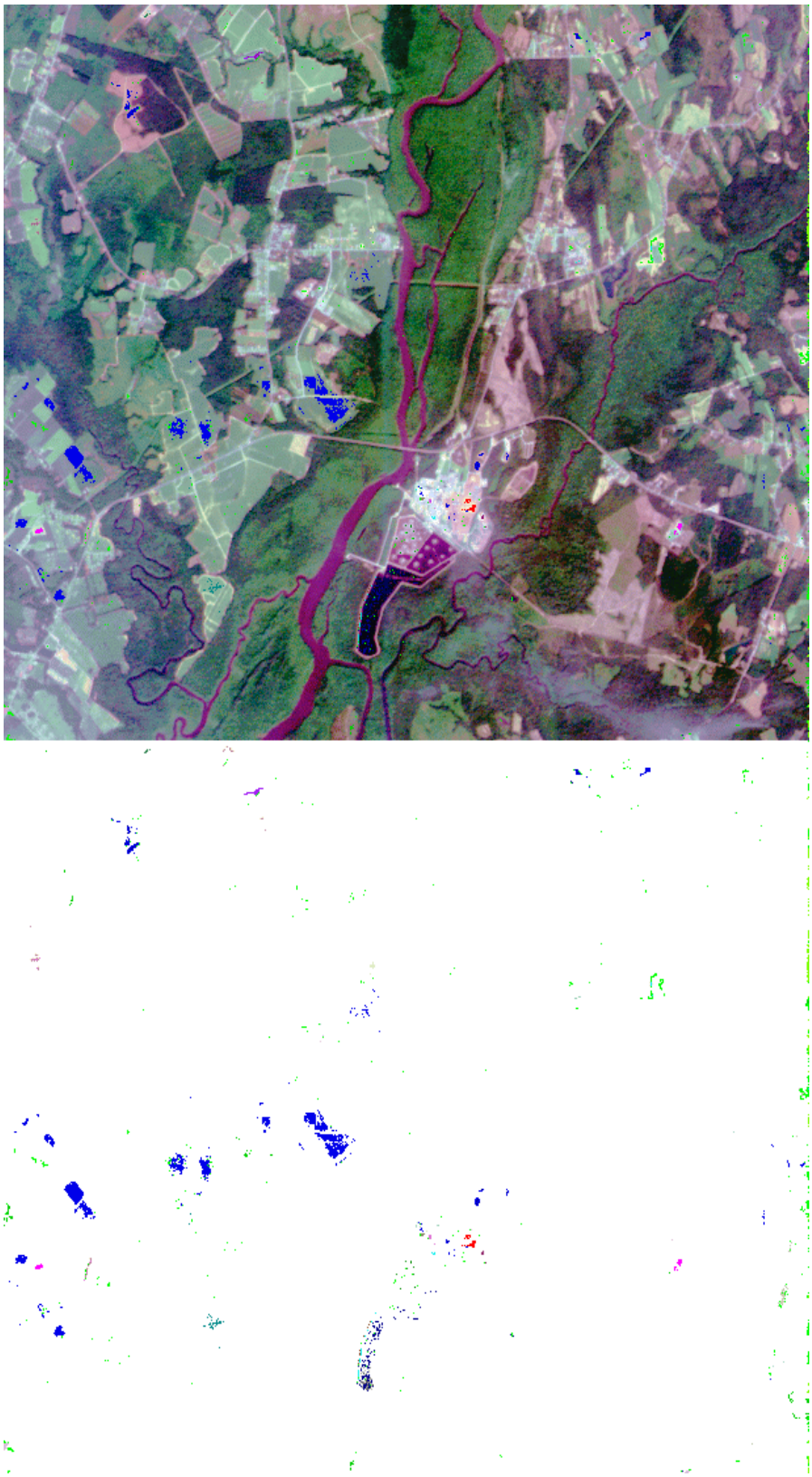

Figure 5. AVIRIS scene f990720t01p02_r02_sc06.v1.img and locations of image endmember pixels. Above: AVIRIS image (visible bands) with endmember pixels plotted. Below: endmember pixels only (image removed).

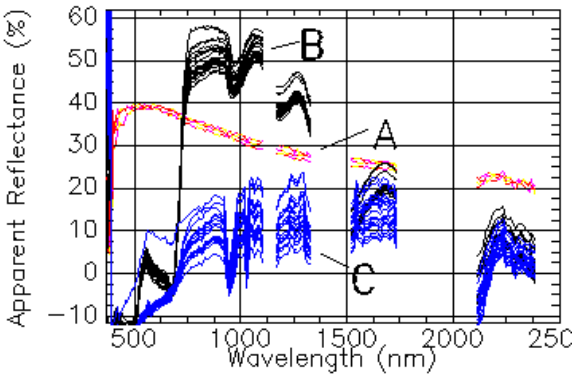

Figure 6. Endmember spectra. A: roof. B: cotton field. C: gravel/soil road.

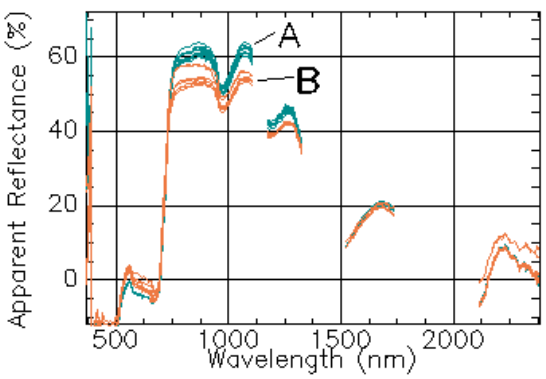

Figure 7. Corn field endmembers.

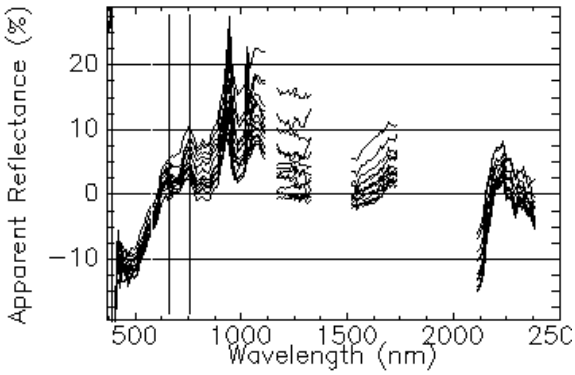

Figure 8. Fallow agricultural field endmember.

(e.g., agricultural fields adjacent to roads, buildings, gravel) (Figs 6.c, 8). At the detailed level (e.g., corn field), no endmembers were purely one crop type.

Three endmembers were labeled edge artifacts. They appeared as a discontinuous column of pixels occupying the right margin of the image (Fig. 5, right margin). Their location and unnatural linear spatial pattern indicated that they did not correspond to any feature of this landscape. Two endmembers were labeled mixed; significantly different land cover classes were contained within a single image endmember (e.g., agriculture and urban). Visual inspection of graphs of all spectra contained in mixed endmembers showed that multiple land cover classes were present (e.g., a group of characteristic vegetation spectra, and another group of characteristic urban spectra). One endmember was labeled woody vegetation, which includes deciduous, evergreen and mixed tree categories. One endmember was labeled water, corresponding to a clear, dark water pond (the water calibration target). One endmember was labeled aerator foam, corresponding to patches of froth and foam around several aerators in a water treatment pond.

5. DISCUSSION

The objective of this experiment was to calibrate an AVIRIS scene, and extract a suite of image endmembers, in preparation for further analysis including spectral unmixing and land cover mapping. The results were encouraging in that the linkages between endmembers and functional land cover classes were reasonably strong, despite a number of potential error sources, which include potential errors in image coregistration, changes in cover type status between the AVIRIS acquisition (1999) and NRB LCLU map (1998-99), the complex nature of vegetation reflectance, and subjectivity in the endmember selection process.

Inspection of spectra at 650 nm shows the endmembers to break into three groups (Fig. 4):

- 40-60 % reflectance, urban (n=4);
- 18-40 % reflectance, urban and mixed (n=8); and
- 0-10% reflectance, vegetation and water (n=13).

Urban endmembers (Group 1) comprised 11 of the 28 endmembers, and were distinct in overall high albedo and rapid increase in blue reflectance. Their relative abundance can be interpreted to mean that urban spectra tend to be more pure than other land cover class spectra in this scene. This results from a number of factors, including the typical spectral homogeneity of urban surfaces, high albedo (thus high signal to noise), and perhaps the fact that urban targets tend to have linear or otherwise distinct (non-diffuse) boundaries (which reduces the effect of intimately mixed pixels). Group 2 endmember spectra showed characteristics of both vegetation and urban spectra. Fallow agricultural fields and farm roads fell in this group, showing contributions from both vegetation and soil components. Vegetation endmembers (Group 3) displayed characteristic green vegetation spectral features: green peak, red edge, infrared plateau, low visible albedo. It is interesting to note that the Neuse River did not produce an endmember, yet it was visually distinct (Fig. 5). The Neuse River is highly turbid with suspended red clay, derived from sediments evident in nearby fields and farm roads. Thus its spectrum is inherently mixed, a combination of water and soil components, and thus less likely to emerge as an endmember in this scene.

Also of interest is the single woody vegetation (i.e., forest) endmember. For our purposes, additional woody vegetation endmembers would be useful in mapping forest associations. Though not strongly expressed in visible wavelengths (Fig. 5), subtle differences in Neuse River flood plain forest areas are well expressed in decorrelation-stretched images for certain wavelength combinations (e.g., 1684, 1614, 1555 nm red, green, blue). The subtle differences among forest pixels were lost in this analysis, overwhelmed by the greater magnitude differences (spectral separability) between urban and vegetation pixels. In order to better extract endmembers for forest pixels, image segmentation is required. By omitting all but forest pixels prior to the MNF transform, the algorithms would operate on a reduced, forest-only set of statistics and produce a different, forest-focused set of endmembers.

The mixed class of endmembers (most apparent in Group 2 spectra) resulted from two primary factors. First, certain pixels are inherently mixed, such as those encompassing both farm roads and adjacent agricultural fields. The second factor was processing related. The interactive grouping of pixels to form endmembers in the n-Dimensional Visualizer™ has inherently subjective components. Results depend on the combination of input bands used, and the analyst's visual perception of relationships among pixels in the animated scatterplot. This step can be refined heuristically as the analyst develops skill through multiple iterations of the technique.

6. CONCLUSIONS

An AVIRIS scene of a densely and diversely vegetated area in the Neuse River Basin of the North Carolina coastal plain was calibrated to apparent reflectance using field acquired reference spectra, and processed to yield 28 image endmembers. The composition of each endmember was identified using an independently-developed NRB LCLU map, in parallel with visual analysis of the original AVIRIS scene. Urban endmembers were the most abundant, followed by agriculture, edge artifacts, mixed, woody vegetation and water. The entire scene was input for processing, and this population of pixels influenced the nature of the output endmembers. If additional endmembers are desired from a particular cover type (e.g., forest), image segmentation to isolate pixels of only that cover class should be performed prior to the MNF transform step. Also, the identity and purity of endmembers are influenced by the band combinations used in the n-Dimensional Visualizer™, and the analyst's visual perception of relationships among pixels. Analyst experience with this step plays a role in endmember extraction.

7. ACKNOWLEDGMENTS

The authors thank Brad Chesson of Weyerhaueser and Clifford Lee of Dupont for assistance in accessing field spectra collection sites, Jayantha Ediriwickrema for land cover data, Jill Crotwell for assistance in image rectification, Dr. Mark Karaska of Applied Analysis, Inc. for assistance in the data acquisition, and the NASA-JPL AVIRIS team for their ongoing efforts.

8. REFERENCES

Boardman, J.W., and F.A. Kruse, 1994. “Automated spectral analysis: a geologic example using AVIRIS data, north Grapevine Mountain, Nevada”. Proceedings, Tenth Thematic Conference on Geologic Remote Sensing, Environmental Research Institute of Michigan, Ann Arbor, Michigan. I- 407-418.

ENVI, 1999. ENVI Tutorials: “Chapter 11, Advanced Hyperspectral Analysis”. Better Solutions Consulting, Inc, Boulder, CO, p. 261-286.

Farrand, W.H., R.B Singer, and E. Merenyi, 1994. “Retrieval of apparent surface reflectance from AVIRIS data: a comparison of empirical line, radiative transfer, and spectral mixture methods”. Remote Sensing of Environment, 47, 311-321.

Green, A.A., M. Berman, P. Switzer, and M. Craig, 1988. “Transformations for ordering multispectral data in terms of image quality and implications for noise removal”. IEEE Transactions on Geoscience and Remote Sensing, 28(1), 65-74.

Green, R.O., M.L. Eastwood, C.M. Sarture, T.G. Chrien, M. Aronsson, B.J. Chippendale, J.A. Faust, B.E. Pavri, C.J. Chovit, M. Solis, M.R. Olah, and O. Williams, 1998. “Imaging spectroscopy and the Airborne Visible/Infrared Imaging Spectrometer (AVIRIS)”. Remote Sensing of Environment, 65, 227-248.